Journal of Molecular Catalysis A: Chemical 356 (2012) 100–105

Contents lists available at SciVerse ScienceDirect

Journal of Molecular Catalysis A: Chemical

journal homepage: www.elsevier.com/locate/molcata

IR characterization of propane oxidation on Pt/CeO_2–ZrO_2: The reaction mechanism and the role of Pt

Bin Wang[a], Xiaodong Wu[a], Rui Ran[a], Zhichun Si[b], Duan Weng[a,b,*]

[a] State Key Laboratory of New Ceramics & Fine Process, Department of Materials Science and Engineering, Tsinghua University, Beijing 100084, China
[b] Advanced Materials Institute, Graduate School at Shenzhen, Tsinghua University, Shenzhen 518055, China

ARTICLE INFO

Article history:
Received 21 June 2011
Received in revised form 19 October 2011
Accepted 31 December 2011
Available online 8 January 2012

Keywords:
Propane oxidation
Pt
CeO_2–ZrO_2 mixed oxides
IR
Mechanism
Adsorption

ABSTRACT

In order to investigate the reaction pathway of propane total oxidation on Pt/CeO_2–ZrO_2 (Pt/CZ) catalyst and the promoting effect of Pt, CeO_2–ZrO_2 (CZ) mixed oxides were prepared by sol–gel method and Pt was impregnated. The catalysts were characterized by means of XRD, BET, TPR, in situ FTIR spectroscopy of propane adsorption/transformation/desorption and propane catalytic oxidation activity experiments. The propane oxidation activity is greatly enhanced by the addition of Pt while there is no obvious structure change based on XRD and BET. It is shown by the adsorption experiments that at 250 °C, propane can react with oxygen-containing species; there is obvious destruction of Ce—O bonds, from which oxygen consumption can be inferred, on both CZ and Pt/CZ catalysts, as well as the generation of some bicarbonate ions on CZ and carbonate on Pt/CZ. Moreover, there are more δ(CH) and δ(CH_2) species on CZ than Pt/CZ. When oxygen was introduced into the reactor, the Ce—O bonds re-formed immediately on Pt/CZ but not on CZ. The propane desorption results show that the intermediate products and desorption process are almost the same on both catalysts. Furthermore, some bidentate carbonate has been detected on both catalysts during the total oxidation process, and it is thought to be the intermediate product of the reaction. Based on the IR results, a possible propane oxidation pathway and the role of Pt as well as the possible electrochemical mechanism have been proposed.

1. Introduction

Catalytic oxidation of hydrocarbons has become the focus of many basic and applied catalysis studies because of its increasing importance for many industrial processes: the production of energy (e.g., gas turbines) and reducing emissions (e.g., automotive exhausts) [1–5], especially in the Partial Oxidation Combustion (POC) of hydrocarbons [6–8]. Many catalysts were developed and show high activity in propane oxidation, such as Au/CuO_x–MnO_x [9], RuO_x/γ-Al_2O_3 [10], and Co_3O_4 [11]. Some materials such as TiO_2, CeO_2, and Al_2O_3 have been compared in order to find an appropriate support for hydrocarbon oxidation [12,13]. Zaki et al., has researched propane oxidation activity of CeO_2, TiO_2 and ZrO_2. CeO_2 showed the best activity, and it is considered a promising material for potential oxide catalysts for the total oxidation of hydrocarbons [14].

With the development of the catalysts, understanding the reaction mechanism of hydrocarbon oxidation becomes a key issue, and some basic work has been done. Andreas Hinz et al., investigated the reaction pathways of propane oxidation on Pt/Al_2O_3 and Pt–SO_4^{2-}/Al_2O_3 using a Temporal Analysis of Products (TAP) reactor system for transient experiments, and the products were detected by mass spectroscopy (MS). The article showed that the presence of SO_4^{2-} results in the breaking of a carbon—carbon bond of propane and causes a change in the reaction mechanism [15]. Faria et al., used in situ Diffuse Reflectance Infrared Fourier Transform Spectroscopy (DRIFTS) to explore the catalytic oxidative steam reforming of propane on Pd/Al_2O_3 and $Pd/CeO_2/Al_2O_3$ and found that a $HCOO^-$ (formate) mechanism is active on Pt/Al_2O_3 but a m-CO_3^{2-} (carbonate) mechanism on $Pt/CeO_2/Al_2O_3$ [16]. Some authors also studied the reaction mechanism with X-ray Absorption Near Edge Spectroscopy (XANES), and some information about catalyst structure and chemical change in the reaction has been obtained [5,17]. Considering all the in situ methods to investigate the reaction mechanism, infrared spectroscopy (IR) is a relatively useful way, since the intermediate products can be directly detected.

In industrial catalysis, precious metals (PM), such as Pd, Pt, Rh, are essential in hydrocarbon oxidation. In order to decrease the use of PM and considering its high price, it is important to understand the reaction mechanism and how PM works in the reaction. The effectiveness of PM may be caused by the high redox ability of PM metal or the metal-support interaction between PM and the support [18], but little is known about the effect of PM addition

* Corresponding author. Tel.: +86 10 62785986; fax: +86 10 62785986.
E-mail address: duanweng@mail.tsinghua.edu.cn (D. Weng).

1381-1169/$ – see front matter © 2012 Elsevier B.V. All rights reserved.
doi:10.1016/j.molcata.2011.12.030

on the propane reaction pathway. Moreover, an electrochemical mechanism has been recently proposed in the propane oxidation on $Pt/Sn_{0.9}In_{0.1}P_2O_7$ catalyst and it shows higher activity compared with the commercial $Pt/\gamma\text{-}Al_2O_3$. $Sn_{0.9}In_{0.1}P_2O_7$ and Pt were used as the proton conductor and electrocatalyst, respectively [4]. Maybe it is the same mechanism on other PM/support catalyst systems and need to be investigated. In order to clarify the effect of PM addition and provide some guide in hydrocarbon oxidation catalyst design, we chose a simple system, CeO_2–ZrO_2 mixed oxides with Pt added by impregnation. Some IR experiments (adsorption, temperature-programmed desorption and in situ reaction) have been carried out and the effect of PM as well as the reaction pathway is discussed.

2. Experimental

2.1. Catalyst preparation

CeO_2–ZrO_2 mixed oxides were synthesized by citric-aided sol–gel method. The nitrates: Ce $(NO_3)_3{\cdot}6H_2O$ and ZrO $(NO_3)_2{\cdot}5H_2O$, were mixed according to the molar ratio of Ce:Zr = 33:67. Citric acid was used as the complexing agent. Appropriate glycol was added, as the dispersant, followed by evaporation and peptization. The sol was heated at 100 °C until a spongy yellow gel remained. Then the gel was decomposed at 300 °C for 1 h and calcinated at 500 °C for 3 h to form CeO_2–ZrO_2 mixed oxides.

The Pt-supported catalysts were prepared by incipient wetness impregnation. Aqueous solutions of Pt $(NO_3)_2$ were used and the nominal loading amount of Pt was 1 wt.%. The impregnated powders were dried at 110 °C overnight and calcined at 500 °C for 3 h to obtain Pt/CZ catalyst. For reference, CZ was also calcinated.

2.2. Catalyst characterizations

The X-ray diffraction analysis (XRD) was conducted on a Japan Science D/max-RB diffractometer employing Cu Kα radiation (λ = 1.5418 Å). The X-ray tube was operated at 45 kV and 150 mA. The X-ray powder diffractograms were recorded at 0.02° intervals in the range $20^\circ \leq 2\theta \leq 80^\circ$ with 0.2 s count accumulation per step. The crystal phase was identified with the help of the JCPDS cards. The calculations and analyses based on the XRD data were assisted by the THX application software.

The specific surface area was determined by the Brunauer–Emmett–Teller (BET) method with an F-sorb 3400 instrument using He as carrier and N_2 as adsorbent.

The H_2 temperature-programmed reduction (H_2-TPR) tests were performed in a fixed-bed reactor with the effluent gases monitored by a mass spectrometer (OmniStar 200). 25 mg of sample were sandwiched by quartz wool and placed in a tubular quartz reactor (i.d. 10 mm). The reactor temperature was raised to 900 °C at a heating rate of 10 °C/min in H_2 (5 vol%)/He (50 mL min^{-1}).

In situ FTIR spectra of adsorption species arising from propane chemisorption at 250 °C were recorded in the range of 4000–650 cm^{-1} using a Thermo Nicolet 6700 FTIR spectrometer equipped with a high temperature environmental cell fitted with a KBr window. Prior to propane chemisorption, the sample was placed in a crucible located in the high-temperature cell and heated up to 500 °C in N_2 flow (100 mL min^{-1}). After the treatment at 500 °C for 30 min, the samples were cooled down to the corresponding temperature, and subsequently, flushed by 100 mL min^{-1} N_2 for 30 min to remove the physisorbed molecules for background collection. Then, the gas mixture containing 800 ppm C_3H_8 in N_2 (100 mL min^{-1}) was passed through the sample at 250 °C for 30 min. The FTIR spectra were collected every 5 min.

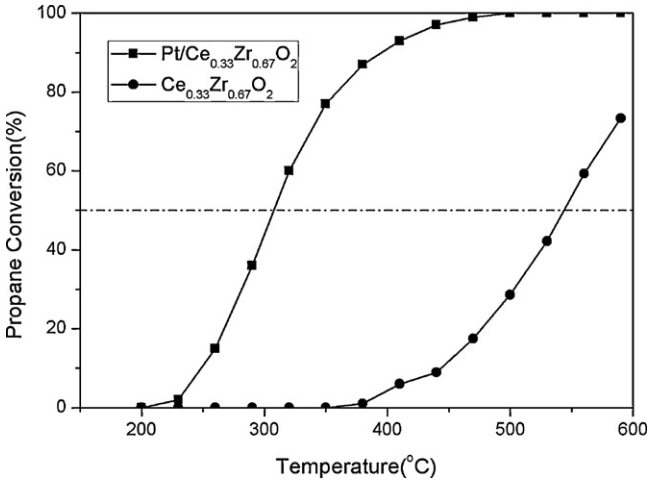

Fig. 1. Light-off curves of propane oxidation over the catalysts. Reaction conditions: 800 ppm C_3H_8/2%O_2/N_2, flow rate = 1000 mL min^{-1}.

The TPD experiments were performed on the same Thermo Nicolet 6700 FTIR spectrometer. The sample powders were first purged in situ in a N_2 stream (100 mL min^{-1}) at 500 °C for 30 min. The background spectra were taken in N_2 atmosphere from 50 to 500 °C at an interval of 50 °C. After that, at room temperature, 800 ppm C_3H_8/N_2 was fed at a flow rate of 100 mL min^{-1} for 30 min and pure N_2 was introduced to remove any physisorbed molecules afterwards. The spectra were determined by accumulating 32 scans at a resolution of 4 cm^{-1}. Then the sample spectra were taken from 50 to 500 °C at an interval of 50 °C in 5% O_2/N_2 atmosphere at a heating rate of 10 °C/min.

The IR experiment of the reaction pathway was also recorded on the Nicolet 6700 spectrometer. The sample powders were purged in situ in a N_2 stream (100 mL min^{-1}) at 500 °C for 30 min. The background spectra were taken in N_2 atmosphere from 50 to 500 °C at an interval of 50 °C. After that, a gas mixture of 800 ppm C_3H_8/2% O_2/N_2 was fed at a flow rate of 100 mL min^{-1}. The spectra were determined by accumulating 32 scans at a resolution of 4 cm^{-1} as a function of temperature at a heating rate of 10 °C/min.

2.3. Activity measurement

The catalytic activity for propane oxidation was tested in a fixed bed reactor made of stainless steel (i.d. 18 mm). 0.2 g of catalyst powders (diluted by coarse quartz particles to 1 mL), sandwiched between two quartz wool layers, were inserted into the reactor. After a pretreatment at 500 °C in N_2 for 30 min and cooling down to RT, the reactor was then heated in the designed gas mixture from RT to 600 °C at a rate of 10 °C/min. The gas mixture consisted of 800 ppm C_3H_8, 2% O_2 and N_2 in balance with a total flow of 1 L min^{-1} and GHSV of 60,000 h^{-1}. The outlet gas concentrations were determined by a Thermo Nicolet 380 IR spectrometer.

3. Results

3.1. Propane oxidation activity

The activity of propane oxidation over CeO_2–ZrO_2 mixed oxides and Pt/CZ catalyst is shown in Fig. 1. CO_2 was the only product detected and the carbon balance was closed, as it was ca. 100%. It can be seen that Pt modification leads to a significant improvement in the propane oxidation activity. The light-off temperatures (T_{50}) are 310 °C (Pt/CZ) < 550 °C (CZ). The shift of T_{50} is more than 200 °C.

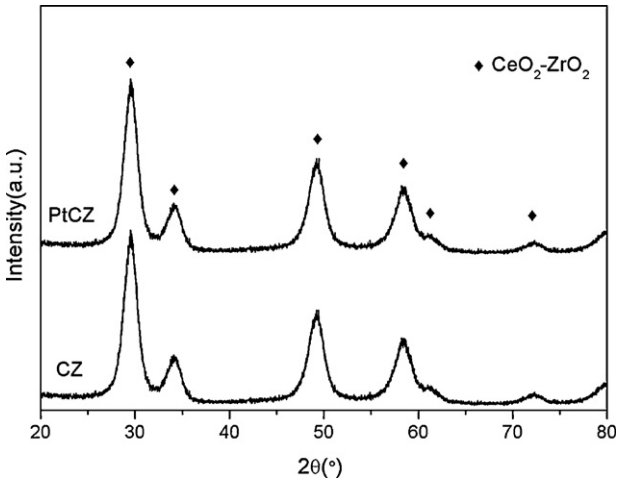

Fig. 2. XRD patterns of CZ and Pt/CZ catalysts.

3.2. Structure characterization

XRD and BET experiments were carried out to characterize the structure of both catalysts. There is no obvious change of the XRD pattern after Pt impregnation and no diffraction peaks of Pt or PtO are found (Fig. 2). Meanwhile, the BET surface area is almost the same; it only changes from 40 m^2/g to 38 m^2/g after Pt impregnation.

3.3. IR characterization

3.3.1. Propane adsorption and reaction at 250 °C

The spectra of propane adsorption on CZ and Pt/CZ catalysts are shown in Fig. 3. It can be seen that when both the catalysts came in contact with propane, the spectra were modified simultaneously, which indicates that some reaction occurred. On the CeO_2–ZrO_2 mixed oxides (Fig. 3 (a)), the negative peak at 3766 cm^{-1} is assigned to terminal Zr—OH and the peak at 3681 cm^{-1} is assigned to terminal Ce—OH groups[14]. With the increase of contact time, these peaks became intensified. Bands around 2970 cm^{-1} are usually attributed to gaseous propane [17,18]. The band at 2870 cm^{-1} (ν_{C-H}) is characteristic of the stretching vibrations of C—H bond, probably CH_2 (ads) and CH_3 (ads) species[14,16], which proves that propane can be cracked on CeO_2–ZrO_2 mixed oxides at this temperature. Besides these peaks, some peaks from 800 to 1700 cm^{-1} occurred and increased with time. These peaks were found at 1612, 1440, 1425, 1331, 1060, 852 cm^{-1}, with a broad peak at 1503 cm^{-1} and a negative peak at 1022 cm^{-1}. The bands at 1425, 1331 and 852 cm^{-1} can be assigned to and ν (CH) species [14]. The peaks at 1440 and 1612 cm^{-1} can be assigned to the bicarbonate ions [19]. The broad and intense band near 1060 cm^{-1} and the apparent 'negative' band at 1022 cm^{-1} observed in all spectra are due, respectively, to the H-bonded hydroxyl groups [20], which are formed upon the reaction ('the positive band'), and the consumption of surface Ce—O—Ce bridges which are perturbed or opened upon surface hydroxylation [21].

With the addition of Pt, the peaks' positions and intensities changed greatly (Fig. 3(b)). The peak at 3749 cm^{-1} became much weaker and the peak at 3681 cm^{-1} nearly disappeared, while, the peak at 2870 cm^{-1} assigned to (d_{C-H}) became much weaker. The exceptions are the bands at 1060 and 1022 cm^{-1} which also occurred in Fig. 3(a) and some new bands at 1630, 1410, 1220, 1135 and 825 cm^{-1}. These peaks at 1135, 1220 and 1410 cm^{-1} are assigned to be bidentate carbonates or some COO^- species. The band at 825 cm^{-1} is related to the COO^- species. The formation of

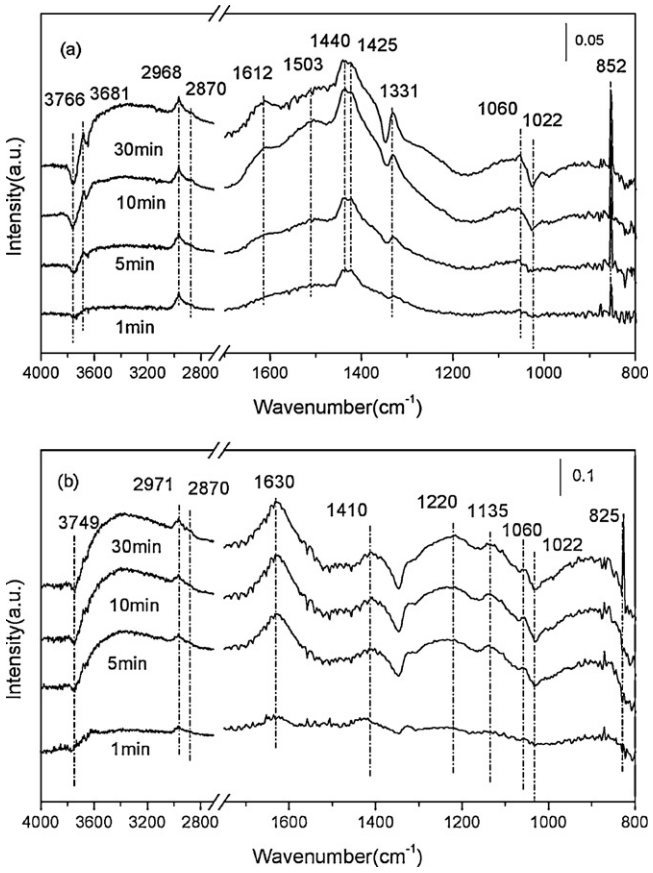

Fig. 3. Propane adsorption and reaction at 250 °C on both catalysts: (a) CZ and (b) Pt/CZ; preadsorption condition: 800 ppm C_3H_8/N_2 for 30 min at 250 °C, flow rate = 100 mL min^{-1}.

water, evidenced by the band at 1630 cm^{-1}, also proves that the total oxidation reaction occurs but not on CZ.

In order to further investigate the propane adsorption species on both catalysts, O_2 was introduced in and the results are shown in Fig. 4. For the two samples, when propane was shut off and O_2 purged in, the band at 2970 cm^{-1} disappeared simultaneously. It can be seen that compared with CZ, more obvious variations of bands were observed on Pt/CZ. The bands at 825 and 1135 cm^{-1}

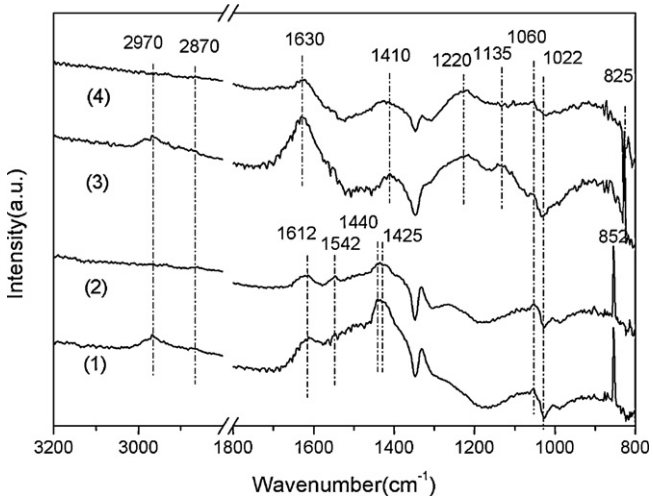

Fig. 4. IR spectra of the adsorbed species from contact with propane on: (1) CZ and (3) Pt/CZ catalysts at 250 °C and then purging with oxygen on: (2) CZ and (4) Pt/CZ.

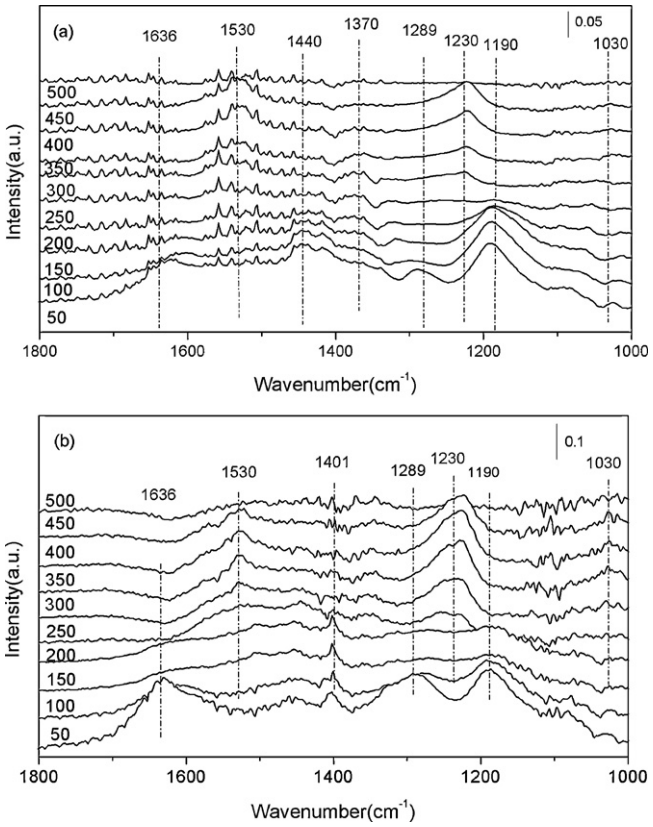

Fig. 5. Propane temperature-programmed desorption in $N_2 + O_2$ atmosphere on both catalysts: (a) CZ and (b) Pt/CZ; preadsorption condition: 800 ppm C_3H_8/N_2 for 30 min at room temperature, flow rate = 100 mL min^{-1}; TPD condition: 5%O_2/N_2, flow rate = 100 mL min^{-1}.

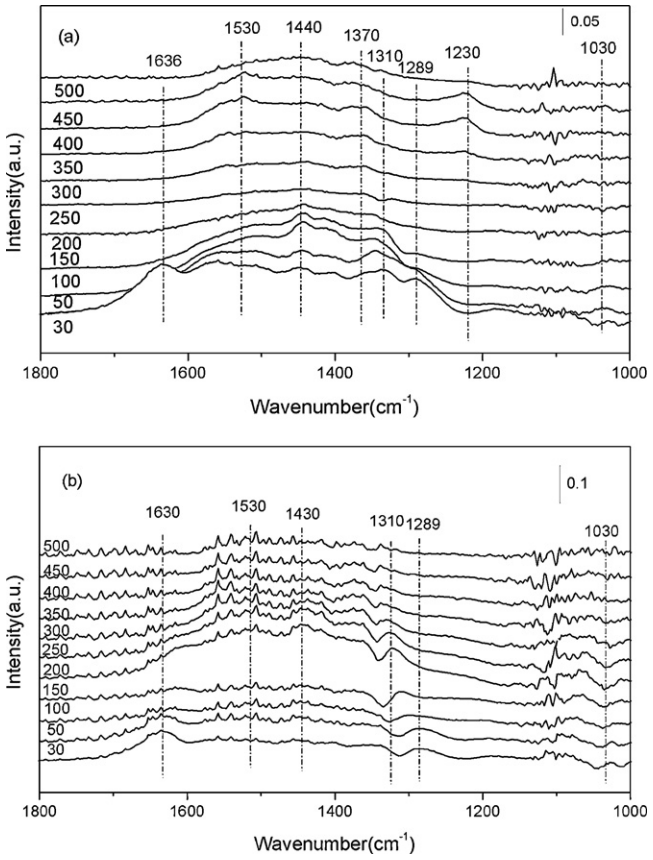

Fig. 6. $C_3H_8 + O_2$ reaction detected by IR on: CZ (a) and Pt/CZ (b). Reaction conditions: 800 ppm $C_3H_8 + 2\%O_2/N_2$, flow rate = 100 mL min^{-1}.

disappeared when O_2 was purged in, while the intensity of the peak at 1022 cm^{-1} became much weaker, which means that the oxygen from the Ce—O bonds was replenished in the oxidation process. The intensity of other peaks at 1630, 1410, 1220 cm^{-1} also became slightly weaker. For the CZ catalyst, there is not much change after O_2 is purged in, which means that little reaction happens. It should be noted that there is no change at the peak of 1022 cm^{-1}.

3.3.2. TPD in $N_2 + O_2$ atmosphere

In order to understand how the propane-adsorbed species transform and the effect of Pt addition, propane-TPD experiments in $N_2 + O_2$ atmosphere were carried out and the results are shown in Fig. 5. For both catalysts, some peaks occurred when propane was purged in even at RT and existed after N_2 was flushed for 30 min; moreover, the peaks seem alike for both samples. The peak at 1636 cm^{-1} is assigned to δ(HOH) vibration of adsorbed water and disappeared when temperature was higher than 100 °C. The peaks at 1289 cm^{-1} and 1190 cm^{-1} are due to C—C bond [22]; the intensity became weaker with increasing temperature and disappeared when the temperature was higher than 250 °C. Peaks assigned to bidentate carbonate are at 1530, 1230 and 1030 cm^{-1} and may indicate the transformation from C—C bonds to carbonates. It is interesting that for both samples the adsorbed species at RT, the extinction temperature of C—C and the transformation to bidentate carbonates are all alike, which may indicate that the transformation and desorption process is mainly related to CeO_2–ZrO_2 mixed oxides.

3.3.3. $C_3H_8 + O_2$ reaction

In order to investigate the reaction pathway on both catalysts, propane and O_2 co-adsorption experiments were carried out and the results are shown in Fig. 6. It can be seen that for both samples at the low temperature, some peaks occurred at 1320, 1289, 1190 cm^{-1} and these species can be assigned to some C—H, and C—C species, as in Fig. 5. As the temperature increases, the intensities of these peaks decrease. When the temperature reached 400 °C, some bidentate carbonate species (1030, 1230 and 1530 cm^{-1}) appeared for CZ, while on the Pt–CZ catalyst, the appearance of these bicarbonate species is in the 200–250 °C temperature region, which is consistent with the activity results. Since the oxidation reaction on Pt/CZ is more violent, compared with CZ, there are more intermediate products observed and the peaks are hard to assign. It could be concluded that the appearance of bidentate carbonate species is a mark of the propane oxidation and the bidentate carbonate species could be considered as the intermediate species.

4. Discussion

4.1. The propane oxidation pathway

Based on the above IR results and precious publications [14–16], the effect of Pt addition on the propane oxidation has been clarified: it speeds up the H—C crack process and promotes the reaction from CH_z to carbonate, and, the oxidation of Ce^{3+} to Ce^{4+} is accelerated by Pt. However, the desorption process mainly relates to the CeO_2–ZrO_2 support. The possible propane oxidation process on CZ and Pt/CZ catalysts may be as follows and the reaction models are also shown in Fig. 7:

Reaction mechanism on Pt/CZ:
Step 1—hydrocarbon cracking.

$$C_3H_8 \rightarrow C_3H_z \rightarrow 3CH_z(ads)(Ptmetal) \quad (1)$$

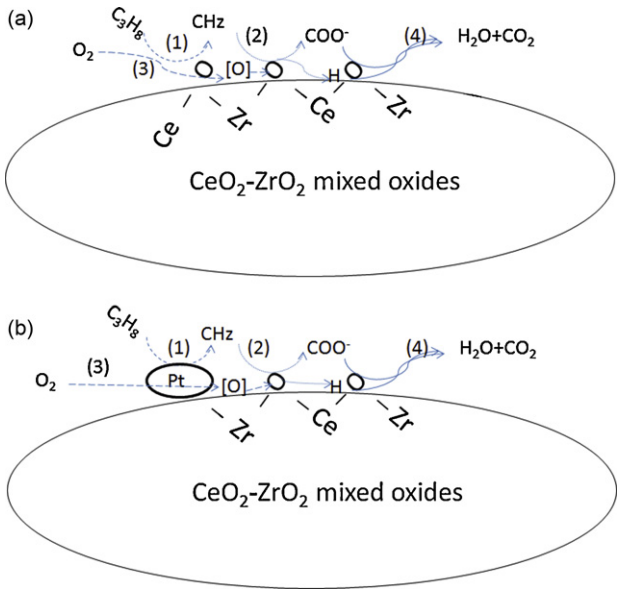

Fig. 7. Propane oxidation reaction scheme on: CZ (a) and Pt/CZ (b).

Step 2—reaction between CH_z fragments and oxygen from support.

$$CH_z(ads) + (4+z)Ce^{4+} + 3O^{2-} \rightarrow CO_3{}^{2-} + (4+z)Ce^{3+} + zH^+ \quad (2)$$

Step 3—oxygen supply.

$$O_2 \rightarrow 2[O](Ptmetal) \quad (3)$$

Step 4—carbonate decomposition under oxidative environment and ceria reoxidation.

$$CO_3{}^{2-} + (4+z)/2[O] + zH^+ + (4+z)Ce^{3+} \rightarrow CO_2 + 0.5zH_2O + (4+z)Ce^{4+} + 3O^{2-}(Ceria) \quad (4)$$

Reaction mechanism on CZ:
Step 1—hydrocarbon cracking.

$$C_3H_8 \rightarrow C_3H_z \rightarrow 3CH_z(ads)(Ceria) \quad (5)$$

Step 2—reaction between CH_z fragments and oxygen from support.

$$CH_z(ads) + (4+z)Ce^{4+} + 3O^{2-} \rightarrow HCO_3{}^- + (4+z)Ce^{3+} + (z-1)H^+(Ceria, RT < 400\,^\circ C) \quad (6)$$

$$CH_z(ads) + (4+z)Ce^{4+} + 3O^{2-} \rightarrow CO_3{}^{2-} + (4+z)Ce^{3+} + zH^+(Ceria, RT > 400\,^\circ C) \quad (7)$$

Step 3—oxygen supply.

$$O_2 \rightarrow 2[O](Ceria) \quad (8)$$

Step 4—carbonate decomposition under oxidative environment and ceria reoxidation.

$$CO_3{}^{2-} + (4+z)/2[O] + zH^+ + (4+z)Ce^{3+} \rightarrow CO_2 + 0.5zH_2O + (4+z)Ce^{4+} + 3O^{2-}(Ceria) \quad (9)$$

4.2. The effect of Pt in propane cracking and oxidation

The results of propane adsorption on CeO_2–ZrO_2 mixed oxides has shown that propane can be cracked on CZ and these δ(CH_2) and δ(CH) species form as well as some bicarbonate at 250 °C.

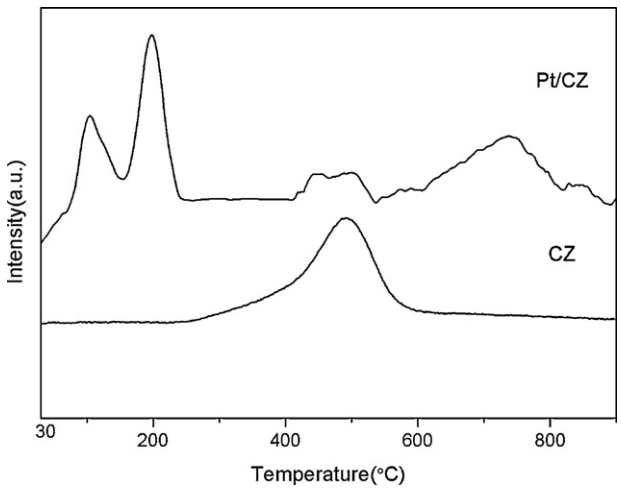

Fig. 8. TPR results of CZ and Pt/CZ.

Moreover, the destruction of Zr—OH bond as well as the formation of Ce—OH bonds can also be detected, which is related to the adsorption of propane and surface reaction. The Ce^{4+}–Ce^{3+} should be the main active sites to crack propane, but at 250 °C, the oxygen mobility in CeO_2–ZrO_2 lattice is limited. Therefore, only the active surface oxygen can react with propane while Ce^{3+} cannot be oxidized and/or re-oxidized at this temperature (see in Fig. 3). For this reason, the main product of propane adsorption is bicarbonate and C—H species, and they cannot be oxidized further by Ce^{4+} at this temperature. Even in the oxygen atmosphere, these species are still stable. Since the amount of surface oxygen is limited, the CZ sample does not show oxidation activity at this temperature. These results are consistent with the research of Alexopoulos et al. [5]; that is, the oxidation process of propane is considered to follow a Mars-van-Krevelen scheme, so the oxidation of Ce^{3+} is the key step. In other words, this process and the C—H cracking are the determining processes. A high temperature is needed for Ce^{3+} to be oxidized, so the activity of propane oxidation on CZ is usually well above 350 °C. With the addition of Pt, the consumption of C—H species is greatly enhanced and there is almost no C—H species. However, some COO^- and carbonate form, which means Pt has a high ability to crack C—H and oxidation occurrs. When O_2 was purged in, the intensity of carbonates and COO^- species decreased and eventually disappeared which showed they may be the intermediate species. Also, the negative peak at 1022 cm^{-1} is replenished, which means Ce^{3+}can be oxidized; this is important for the propane oxidation.

CeO_2–ZrO_2 mixed oxides have been widely used in catalysis and solid oxide fuel cells because of its oxygen storage capability. Some oxygen vacancies exist in the CeO_2–ZrO_2 mixed oxides and oxygen ionic can transfer through these vacancies in the lattice. The oxygen mobility and reduction ability of surface oxygen increases obviously with the addition of noble metals, such as Rh, which may benefit from the spillover effect of noble metals [23] and it can also be evidenced by our TPR results in Fig. 8. The reduction peaks for CeO_2–ZrO_2 mixed oxides are higher than 500 °C; with the spillover effect of Pt, the reduction peaks of CeO_2–ZrO_2 partly move to lower temperatures around 200 °C, which proves the enhancement of the oxygen mobility. In this way, the effect of Pt addition in the propane oxidation reaction can be beneficial from the local cell mechanism. CZ and Pt can be regarded as an oxide ion conductor and an electrocatalysis, respectively. Due to the heterogeneity of Pt cluster, both the anodic and cathodic sites are present at the interface of CZ and Pt. At the anodic site, propane or the cracked fragment reacts with oxide ions to form CO_2 and electrons. While the electrons migrate through the Pt cluster from the anodic site to the cathodic site, oxide

ions conduct through CZ from cathodic site to the anodic site. At the cathodic site, oxygen is reduced to oxide ions by the reaction with the electrons. Therefore, these series of reactions are promoted by the presence of Pt on the CZ surface. The detailed electrochemical cell model and the affecting factors will be further investigated in the future.

5. Conclusion

In this study, the effect of Pt addition on the propane oxidation on CeO_2–ZrO_2 mixed oxides and the propane oxidation pathway were investigated. There is no obvious change in the structure with Pt impregnation but the propane oxidation activity improved obviously. IR results suggested that Ce^{4+}–Ce^{3+} pair is the main reaction site on CZ and the reoxidation of Ce^{3+} could be the limiting step. The addition of Pt enhanced the cracking of propane and greatly accelerated the oxidation of Ce^{3+} to allow for regeneration, meanwhile, the activity improvement can also be beneficial from the electrochemical reaction by the presence of Pt on the CZ surface. In addition, some bidentate carbonate species have been detected and are believed to be the intermediate of the propane oxidation reaction, and PM has no significant role in the desorption of these species.

Acknowledgments

The authors would like to acknowledge the Ministry of Science and Technology, PR China for the financial support of Project 2010CB732304, National Natural Science Foundation of China for the financial support of Project 50972069 and financial support from Ministry of Industry and Information Technology, PR China. Moreover, we would also thank the Center of Analysis and Key Lab of Advanced Materials in Tsinghua University.

References

[1] B. Solsona, T. García, G.J. Hutchings, S.H. Taylor, M. Makkee, Appl. Catal. A 365 (2009) 222–230.
[2] L. Zhang, D. Weng, B. Wang, X.D. Wu, Catal. Commun. 11 (2010) 1229–1232.
[3] G. Wang, M. Meng, Y.Q. Zha, T. Ding, Fuel 89 (2010) 2244–2251.
[4] K. Tsuneyama, S. Tetanishi, T. Hibino, S. Nagao, H. Hirata, S.I. Matsumoto, J. Catal. 273 (2010) 59–65.
[5] K. Alexopoulos, M. Anilkumar, M.F. Reyniers, H. Poelman, S. Cristol, V. Balcaen, P.M. Heynderickx, D. Poelman, G.B. Marin, Appl. Catal. B 97 (2010) 381–388.
[6] X.D. Yi, X.B. Zhang, W.Z. Weng, H.L. Wan, J. Mol. Chem. A 277 (2007) 202–209.
[7] Cimino, F. Donsì, G. Russo, D. Sanfilippo, Catal. Today 157 (2010) 310–314.
[8] Y.M. He, Y. Wu, X.D. Yi, W.Z. Weng, H.L. Wan, J. Mol. Chem. A 331 (2010) 1–6.
[9] B. Solsona, T. Garcia, S. Agouram, G.J. Hutchings, S.H. Taylor, Appl. Catal. B 101 (2011) 388–396.
[10] J. Okal, M. Zawadzki, W. Tylus, Appl. Catal. B 101 (2011) 548–559.
[11] T. Garcia, S. Agouram, J.F. Sánchez-Royo, R. Murillo, A.M. Mastral, A. Aranda, I. Vázquez, A. Dejoz, B. Solsona, Appl. Catal. A 386 (2010) 16–27.
[12] J. Okal, M. Zawadzki, L. Krajczyk, Catal. Today (2011), doi:10.1016/j.cattod.2010.11.096.
[13] P.M. Heynderickx, J.W. Thybaut, H. Poelman, D. Poelman, G.B. Marin, J. Catal. 272 (2010) 109–120.
[14] M.A. Hasan, M.I. Zaki, L. Pasupulety, J. Phys. Chem. B 106 (2002) 12747–12756.
[15] A. Hinz, M. Skoglundh, E. Fridell, A. Andersson, J. Catal. 201 (2001) 247–257.
[16] W.L.S. Faria, C.A.C. Perez, D.V. César, L.C. Dieguez, M. Schmal, Appl. Catal. B 92 (2009) 217–224.
[17] G. Silversmit, H. Poelman, V. Balcaen, P.M. Heynderickx, M. Olea, S. Nikitenko, W. Bras, P.F. Smet, D. Poelman, R.D. Gryse, M.F. Reniers, G.B. Marin, J. Phys. Chem. Solids. 70 (2009) 1274–1284.
[18] C. Bozo, N. Guilhaume, J.M. Herrmann, J. Catal. 203 (2001) 393–406.
[19] K. Pokrovski, K.T. Jung, A.T. Bell, Langmuir 17 (2001) 4297–4303.
[20] J.C. Lavalley, M. Bensitel, J.P. Gallas, J. Lamotte, G. Busca, V. Lorenzelli, J. Mol. Chem. A 175 (1988) 453–458.
[21] V. Ermini, E. Finocchio, S. Sechi, G. Busca, S. Rossini, Appl. Catal. A 190 (2000) 157–167.
[22] E. Finocchil, G. Busaca, V. Lorenzelli, R.J. Willey, J. Catal. 151 (1995) 204–215.
[23] J. Kašpar, P. Fornasiero, M. Graziani, Catal. Today 50 (1999) 285–298.